J. Fluid Mech. (1981), *vol.* 110, *pp.* 273–292
Printed in Great Britain

The effect of base bleed on vortex shedding and base pressure in compressible flow

By F. MOTALLEBI AND J. F. NORBURY
Department of Mechanical Engineering, University of Liverpool,
P.O. Box 147, Liverpool, L69 3BX

(Received 8 September 1980 and in revised form 8 December 1980)

Experiments have been carried out to investigate the phenomenon of vortex shedding from the blunt trailing edge of an aerodynamic body in transonic and supersonic flow. The effect of a discharge of bleed air from a slot in the trailing edge has been included and the relationship between the vortex formation and base pressure has been considered.

In transonic flow a small amount of bleed air was found to produce a rearward shift in the point of origin of the vortices with a consequent substantial increase in base pressure. The effect was less marked in supersonic flow. At higher rates of bleed two different regimes of vortex shedding were identified and increase in bleed rate caused a reduction in base pressure. For bleed rates giving near-maximum base pressure no vortex shedding occurred.

1. Introduction

The base pressure acting on the blunt trailing edge of an aerodynamic body is an important factor in a number of applications. The present work arose from an interest in the losses incurred from this cause in turbine blading, especially when the flow includes a discharge of cooling air from the trailing edge. It forms part of a series of investigations (Abdul-Kadir 1976; Edwards 1980) and is especially concerned with the role of vortex formation in the flow.

Wood (1964) has carried out experiments at low speed on a 9% thick aerofoil and has shown that a decrease in profile drag caused by base bleed was associated with a decrease in the strength of the vortex street formed in the wake. The initial formation of the vortices occurred further downstream as the bleed quantity was increased. Bearman (1967) obtained similar results for two different slots occupying respectively 0·59 and 0·93 of the base height. He found a linear relationship between base pressure coefficient and the inverse of the vortex formation distance, a relationship also applicable when the vortex formation was delayed by a splitter plate rather than by base bleed.

In a series of papers Heinemann, Lawaczeck and Bütefisch (Lawaczek & Heinemann 1975; Heinemann, Lawaczek & Bütefisch 1975; Heinemann & Bütefisch 1978) have described observations of vortex streets in the wake flows behind cascades of turbine blades and of flat plates with rounded trailing edges. The experiments were carried out at outlet Mach numbers ranging from low values to the transonic range, the maximum being about 1·3 for the flat plate cascades. Measurements of vortex-shedding frequency were obtained by a number of techniques including spark–

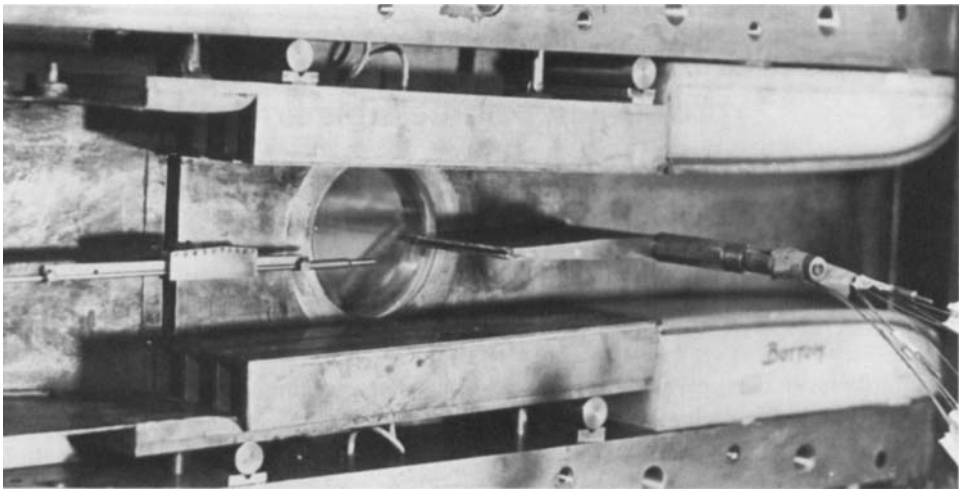

FIGURE 1. Working section of wind tunnel with model in position.

schlieren photography and a photo-multiplier system. Values of Strouhal number, based on trailing-edge thickness and downstream velocity, ranged between 0·17 and 0·4. Apart from some isolated cases the values of Strouhal number varied only slowly with Mach number.

The aerodynamic body used in the present experiment was designed to have variable incidence so that a pressure difference could be established across the rearward part of the profile, as in a turbine blade. However the results to be described were all obtained for nominally symmetrical flow at zero incidence. Attention is principally focused on the relationship between the base pressure and the vortex-shedding phenomenon for transonic and low supersonic mainstream Mach numbers, including especially the effect of the base bleed flow. In the text of the paper the terms 'base' and 'trailing edge' are used synonymously.

2. Experimental facility

2.1. *Transonic tunnel and aerodynamic model*

The test section of the transonic tunnel is nominally 102 × 102 mm with slotted upper and lower surfaces which are adjustable. The tunnel may run continuously, being supplied by air at a total pressure up to 3 atmospheres absolute and with a maximum mass flow of 5 kg s^{-1}. The total temperature and the humidity of the air can both be controlled. The test section is fitted with schlieren windows of diameter 110 mm and the model was positioned so that the flow might be visualized over the downstream part of the model and the first part of the wake. Figure 1 is a photograph illustrating the working section with the model in position.

Some details of the model are shown in figure 2. It had a symmetrical profile designed in a similar way to that of a supersonic tunnel liner to give a uniform and parallel flow approaching the base for a mainstream Mach number of 1·3 (Malhotra 1974). The slot through which the bleed air was discharged occupied the middle one-third of the trailing-edge thickness. The bleed air entered the interior of the model through two air inlet ports, placed one on each side near to the leading edge. The bleed

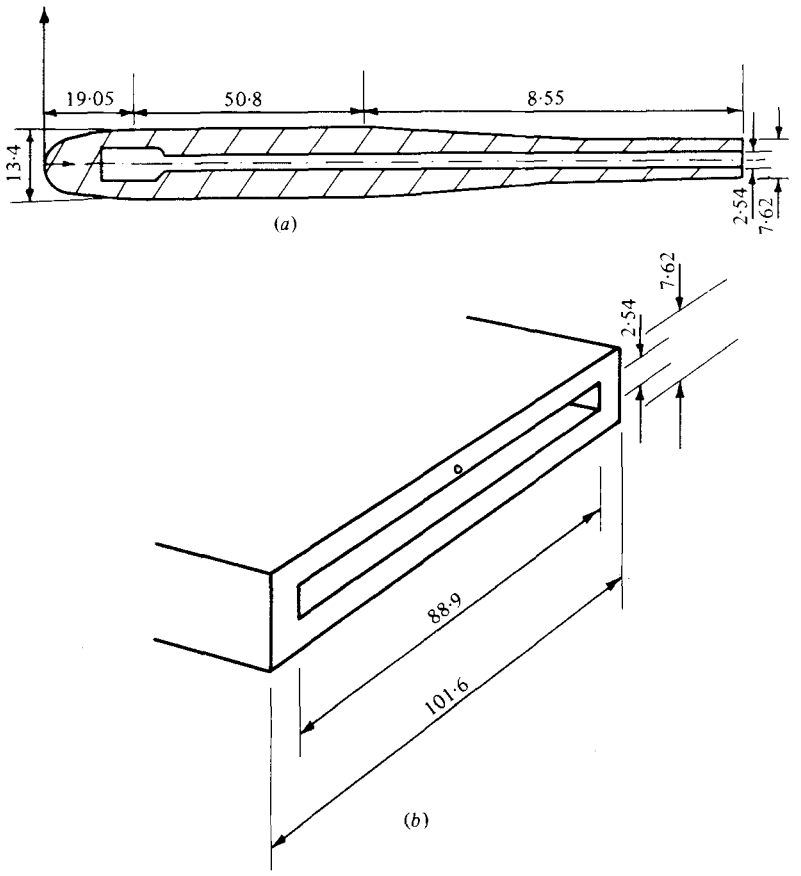

FIGURE 2. Details of model. (*a*) Model cross-section; (*b*) base geometry. (All dimensions are in millimetres.)

air was distributed laterally through the small plenum chamber shown in figure 2 and then passed rearwards through the constant-section duct upstream of the trailing-edge slot. At the trailing edge the distribution of bleed air across the span of the model was reasonably uniform. Across the height of the slot the velocity profile was typical of a fully developed flow.

On the exterior of the profile the transition points of the boundary layers were fixed by means of transition wires of diameter 0·18 mm. These were placed symmetrically on the upper and lower surfaces at a distance of 10 mm from the leading edge.

The base pressure was measured at a single tapping point located 4·8 mm off the spanwise centre-line as shown in figure 2. In earlier experiments Abdul-Kadir (1976) had shown that the same reading could be obtained from a Pitot tube with its mouth placed immediately behind the tapping point. Furthermore by traversing the Pitot tube in a spanwise direction behind the trailing edge he demonstrated that, for the slotted base with zero blowing, the variation of base pressure along the span was small, less than 2% of the mainstream dynamic pressure. These results were considered to confirm a satisfactory two-dimensionality of the flow.

Values of mainstream Mach number, M_∞, were obtained, using a preliminary

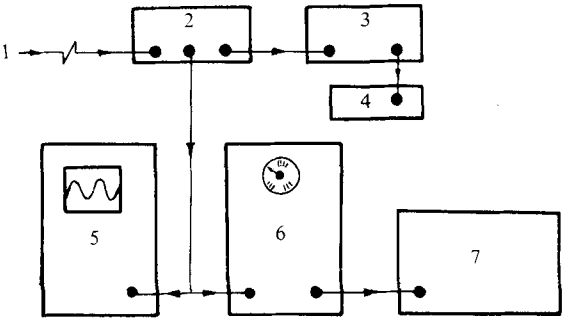

FIGURE 3. Hot-wire equipment. 1, Hot-wire signal; 2, constant-temperature anemometer; 3, true integrator; 4, digital voltmeter; 5, storage oscilloscope; 6, frequency analyser; 7, recorder.

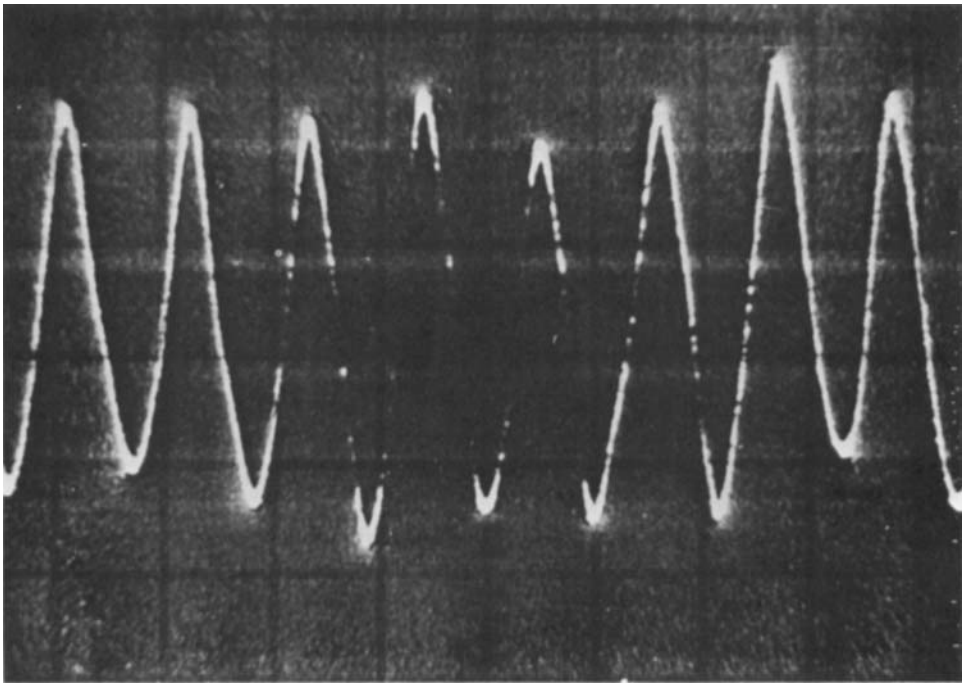

FIGURE 4. Typical hot-wire output signal indicating vortices.

calibration, from static pressure measurements respectively in the upstream settling chamber and in the plenum chambers bounding the slotted walls. In view of the use of slotted walls no correction has been applied for interference effects.

The Reynolds number, based on chord length and mainstream speed, varied from $1{\cdot}6 \times 10^6$ at $M_\infty = 0{\cdot}6$ to 4×10^6 at $M_\infty = 1{\cdot}3$. Corresponding values based on base height are therefore $0{\cdot}8 \times 10^5$ and 2×10^5. It was possible to obtain a limited variation of Reynolds number independent of Mach number by adjustment of the valves upstream and downstream of the working section. Using this technique the Reynolds number was varied from $1{\cdot}6 \times 10^6$ to $2{\cdot}8 \times 10^6$ for $M_\infty = 0{\cdot}6$. Within this range the effect of Reynolds number on base pressure and on Strouhal number was negligible.

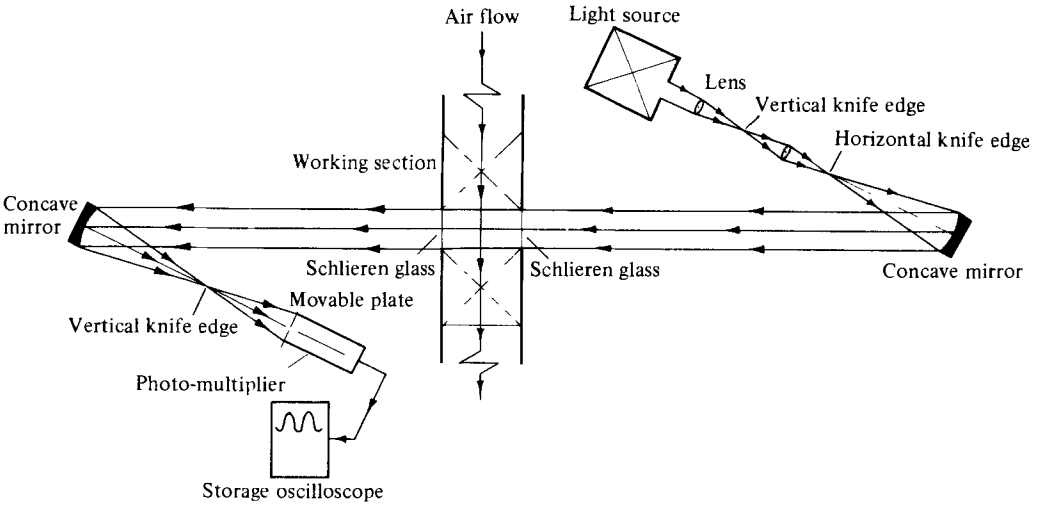

FIGURE 5. Schlieren system with photo-multiplier.

The experiments included a comparison of the flow past the slotted trailing edge (for zero bleed) with that past a solid trailing edge. For this purpose the solid base was obtained by filling the slot with a metal strip.

2.2. *Hot-wire apparatus*

The first attempts to obtain detailed measurements of the flow in the immediate neighbourhood of the trailing edge were made using a standard hot-wire probe (Disa type 55P11, 5 μm). However, the wire was short-lived, probably as a result of contamination by fine particles of oil from the compressor.

The wire was therefore reinforced by introducing a narrow bridge of Araldite immediately behind the wire and spanning the space between the prongs of the probe, a technique developed by Mikulla (1969). In this form the hot wire was used very successfully for long periods. The effect of contamination in changing the calibration precluded its use to measure velocities accurately but it was used quite satisfactorily to obtain the periodic signals generated by shed vorticity and hence to determine the frequency of these.

The complete system is shown in figure 3. However, the frequency analyser and level recorder were only used in the first stages of the experiments. The frequencies obtained from the storage oscilloscope and the frequency analyser gave good correspondence and it was found more convenient to determine the frequency from the stored signals on the oscilloscope screen. Figure 4 shows a typical output signal indicating the passage of vortices.

All measurements were made in the centre-span plane downstream of the trailing edge, the position of the hot wire being varied for each flow regime to obtain the most satisfactory signal.

2.3. *Schlieren apparatus*

A basic schlieren system was used in two different forms. (Actually a third, stroboscopic schlieren system, was also tried but the photographs resulting proved inferior to those obtained from the spark–schlieren system that was eventually adopted.)

In the spark system the light source was an argon arc having time duration of

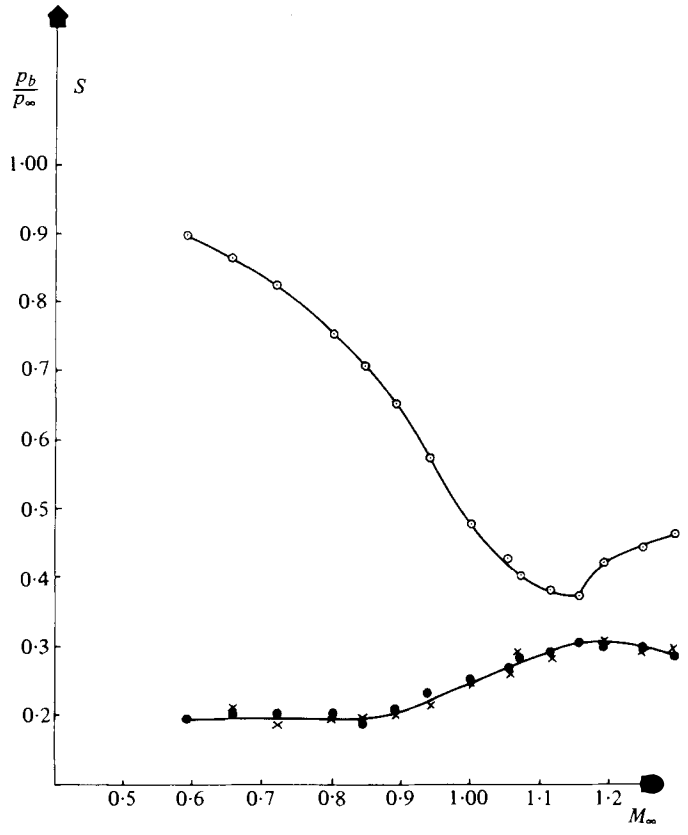

FIGURE 6. Variation of base pressure p_b/p_∞ and Strouhal number, S (vortex-shedding frequency × base height/mainstream flow velocity), with Mach number for solid base. ⊙, p_b/p_∞; ●, S_p; ×, S_h.

about 1 microsecond. This was sufficiently short to give reasonably good indications of the shed vortices.

In order to obtain a supplementary method of determining the frequency of the shed vortices a photo-multiplier system was added to the basic schlieren equipment (figure 5). The photographic plate normally used was replaced by a movable screen with a small orifice of diameter less than 1 mm. A photo-multiplier was placed behind the orifice so as to respond to the variations in illumination occurring periodically as successive vortices passed across the field of view. The output from the photo-multiplier was fed to the storage oscilloscope and the signals recorded by the oscilloscope could then be analysed to obtain the shedding frequency.

3. Experimental results

3.1. *Zero bleed flow*

For the solid base (i.e. with the slot filled by a metal strip) the variation of base pressure with Mach number is shown in figure 6. The figure also shows the values of Strouhal number measured both with the hot-wire system and with the photo-multiplier. The two systems gave results that correspond closely.

The curve of Strouhal number remains at a more or less constant value up to a

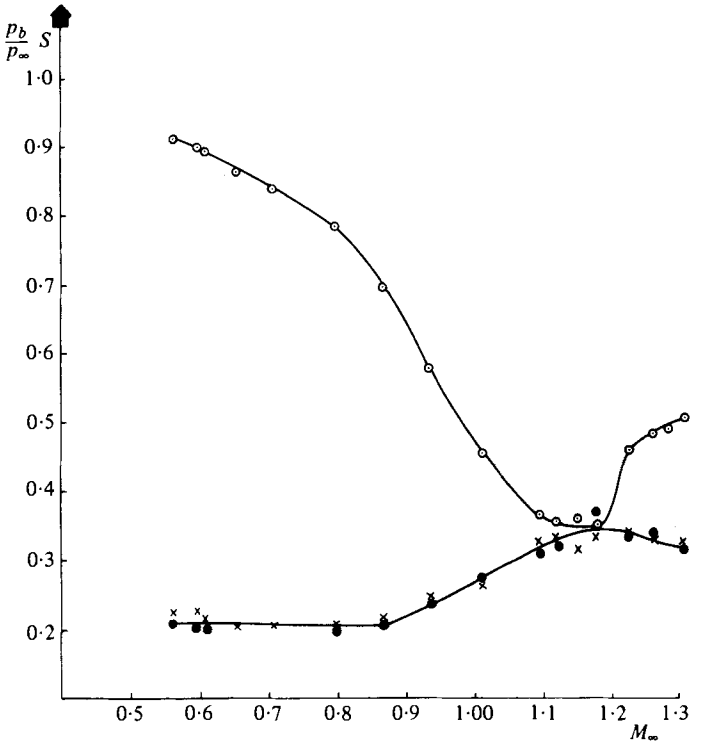

FIGURE 7. Variation of base pressure and Strouhal number with Mach number for slotted base with zero bleed. ⊙, p_b/p_∞; ●, S_p; ×, S_h.

Mach number of about 0·9 and then rises to a maximum value at a Mach number just less than 1·20. This corresponds to the minimum value of the base pressure curve.

Corresponding results for the slotted base with zero bleed flow are shown in figure 7. For values of mainstream Mach number less than 1·0 the results are very similar to those for the solid base, although the measured values of Strouhal number are somewhat higher. At higher values of Mach number there are significant differences between the two sets of curves. The lowest values of base pressure lie below the minimum for the solid base. At first it was believed that this was due to experimental error. Consequently the observations were carried out several times on different occasions. The results were always similar and it is therefore considered that the differences exhibited for $M_\infty > 1$ are correctly represented.

As in the case of the solid base the maximum of the curve of Strouhal number occurs at virtually the same Mach number as the minimum value of the base pressure.

Spark-schlieren photographs of the wake flow for the slotted base are shown in figures 8(*a*, *b*, *c*), for mainstream Mach numbers in the subsonic, transonic and supersonic ranges respectively. The pattern of shed vortices is evident in figure 8(*a*) ($M_\infty = 0{\cdot}68$) which appears to show a vortex just forming immediately behind the trailing edge. The more interesting result for $M_\infty = 1{\cdot}06$ is shown in figure 8(*b*). The Mach number corresponding to the base pressure in this case is 1·7 and the figure shows the region of expansion on either side of the trailing edge. The two shear layers

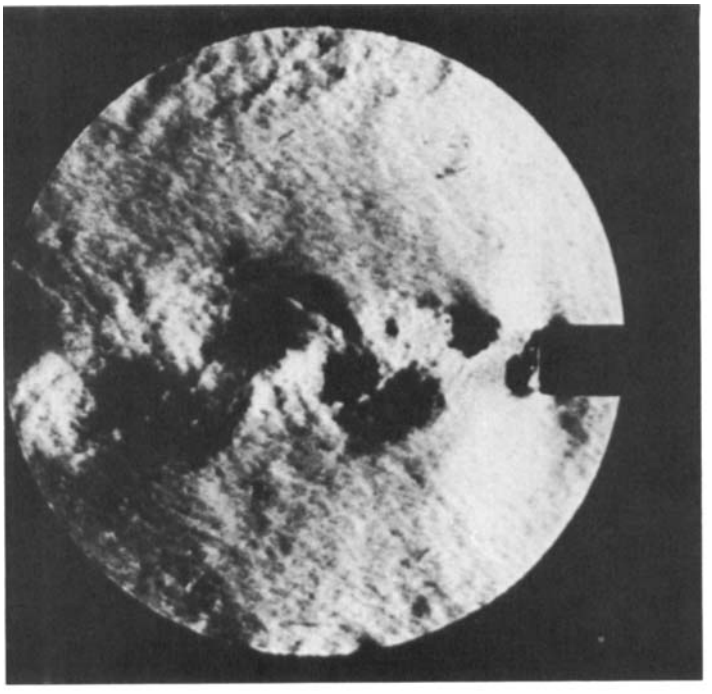

(*a*)

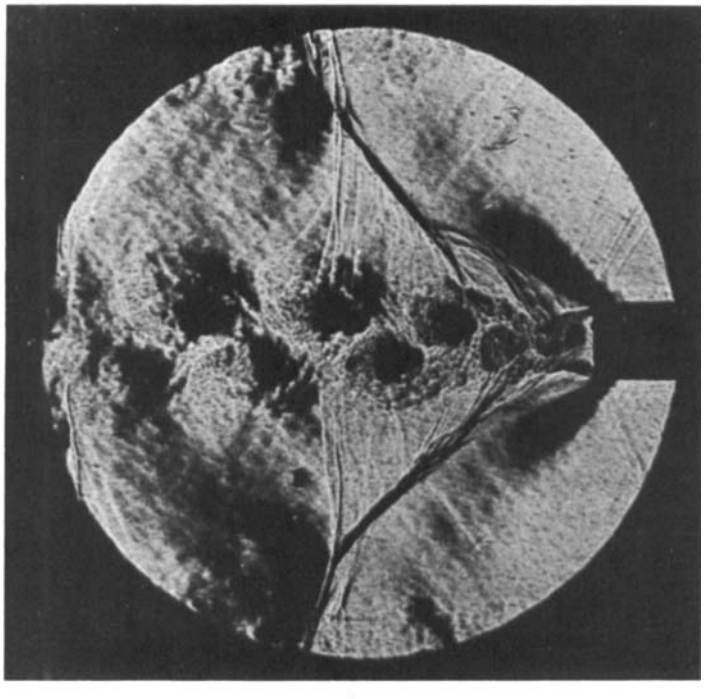

(*b*)

FIGURE 8. Spark–schlieren photographs of wake flow for (*a*) $M_\infty = 0{\cdot}68$; (*b*) $M_\infty = 1{\cdot}06$; (*c*) $M_\infty = 1{\cdot}30$. $C_q = 0$.

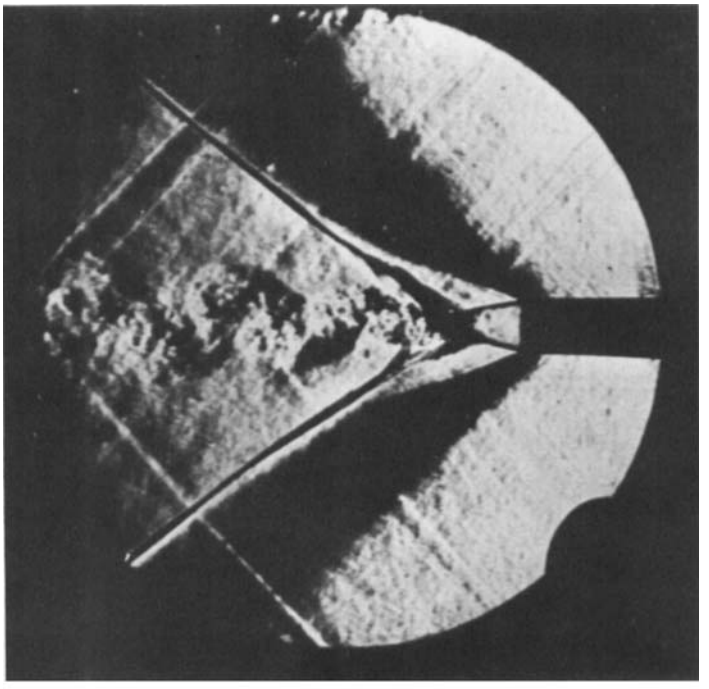

(*c*)

FIGURE 8*c*. For legend see opposite page.

springing from the upper and lower boundaries of the trailing edge appear to enclose the first of the formed vortices. The pair of trailing oblique shocks, which exhibit the diffused lambda-like form typical of a shock wave impinging on a shear layer, converge towards a point downstream of the trailing edge by about one base height. There is, however, the expected asymmetry between the two shocks which oscillate at the frequency of the vortex shedding. Measurements of static pressure distribution along the wake centre-line showed that the steepest pressure rise occurred between 1·5 and 2 base heights downstream of the trailing edge.

Further downstream lies a normal shock which appears to result from interference between the oblique shocks and the shear layers on the slotted walls of the tunnel. However, this normal shock appears to play no significant role in the mechanism of the generation and development of the shed vorticity. The angle at which the shed vortices spread laterally from the wake centre-line is considerably smaller than in the case of the subsonic mainstream flow (figure 8*a*).

The schlieren photograph for the supersonic mainstream flow with $M_\infty = 1{\cdot}30$ is shown in figure 8(*c*). In this case the base pressure corresponds to a local Mach number of nearly 1·9 and large regions of expansion are clearly evident. The region of confluence of the trailing-edge shear layers and the oblique trailing shocks occurs further downstream than in the transonic case and the rate of lateral divergence of the shed vortices is smaller.

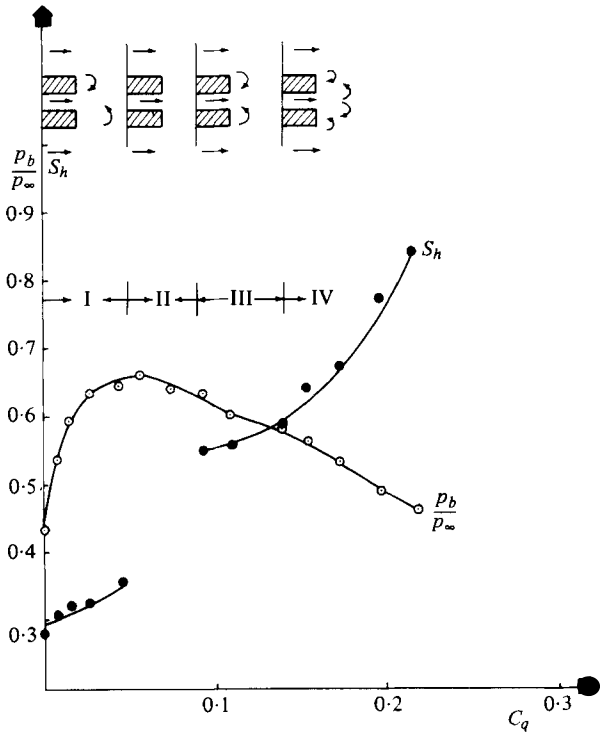

FIGURE 9. Variation of base pressure and Strouhal number with bleed air mass flow for $M_\infty = 1{\cdot}03$.

3.2. *Effect of bleed air*, $M_\infty = 1{\cdot}03$

For transonic mainstream flow the effect of air bled from the trailing edge slot is shown in figure 9 in which the abscissa is a coefficient representative of the rate of mass flow of air through the slot:

$$C_q = \dot{m}/2\rho_\infty U_\infty hl,$$

where $\dot{m}$ is the mass flow rate of bleed air, ρ_∞ and U_∞ are the density and flow velocity in the mainstream, and h and l are the half-height of the base and the span of the model. A comparatively small amount of bleed air produces a substantial increase in the base pressure, which rises from its zero bleed value of 0·43 to a maximum value of 0·66. From this point further increases in the blowing rate produce a continuous reduction in base pressure, the gradient being smaller than that of initial rise.

The smooth variation of the base pressure is by no means reflected in the behaviour of the wake vortex street, for which the variation of Strouhal number is shown in the figure. At rates of blowing up to the rate which produces the maximum value of base pressure there is a small increase in the value of the Strouhal number. There is then a range of blowing rates for which no periodicity can be detected in the wake, the inference being that over this range the phenomenon of periodic vortex shedding does not occur. However at a value of C_q just below 0·1 the occurrence of wake vorticity is resumed. It takes the form of a single vortex train at a frequency almost double that of the frequency for low blowing rates. At still higher blowing rates, beginning at the point at which $C_q = 0{\cdot}14$, the vortex pattern changes again. There are

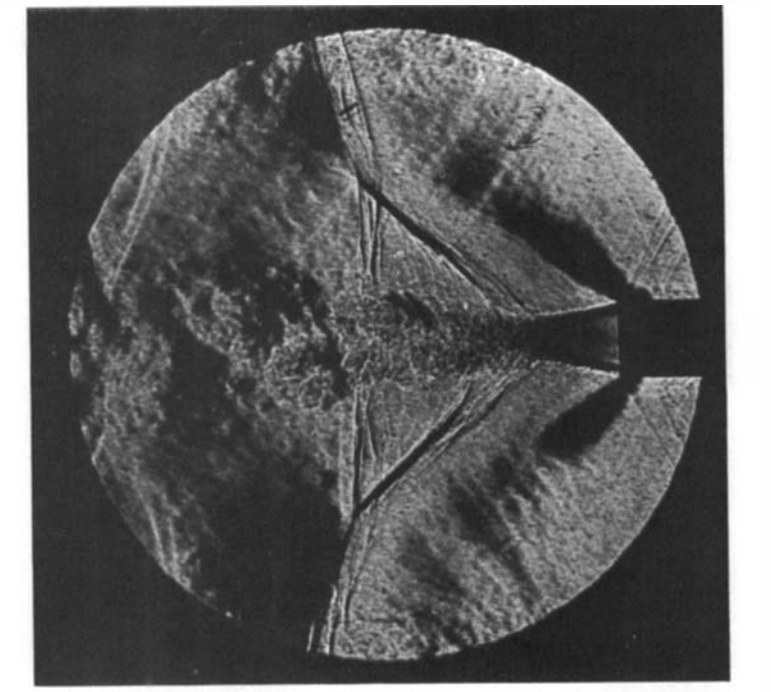

(*a*)

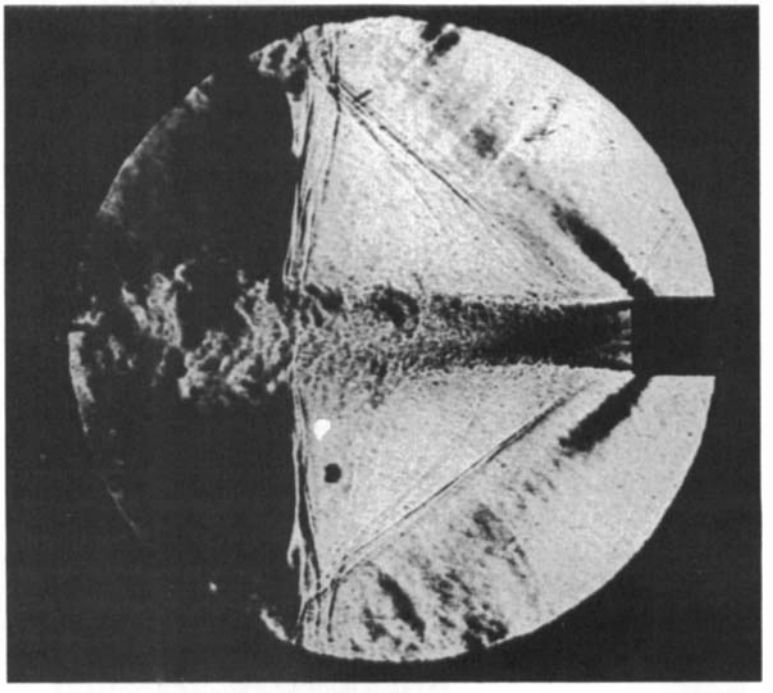

(*b*)

FIGURE 10. Spark-schlieren photographs, $M_\infty = 1{\cdot}06$; (*a*) $C_q = 0{\cdot}009\ 2$;(*b*) $C_q = 0{\cdot}056$; (*c*) $C_q = 0{\cdot}13$; (*d*) $C_q = 0{\cdot}20$.

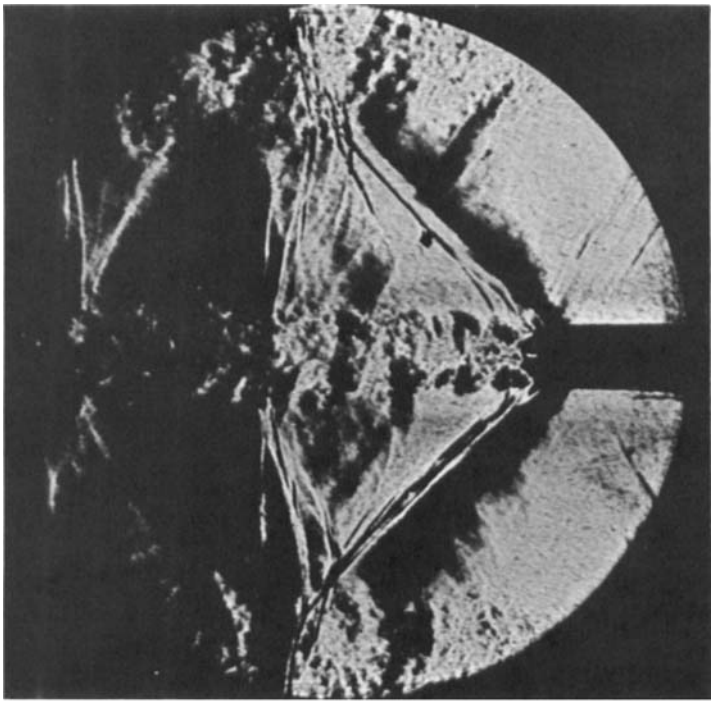

(*c*)

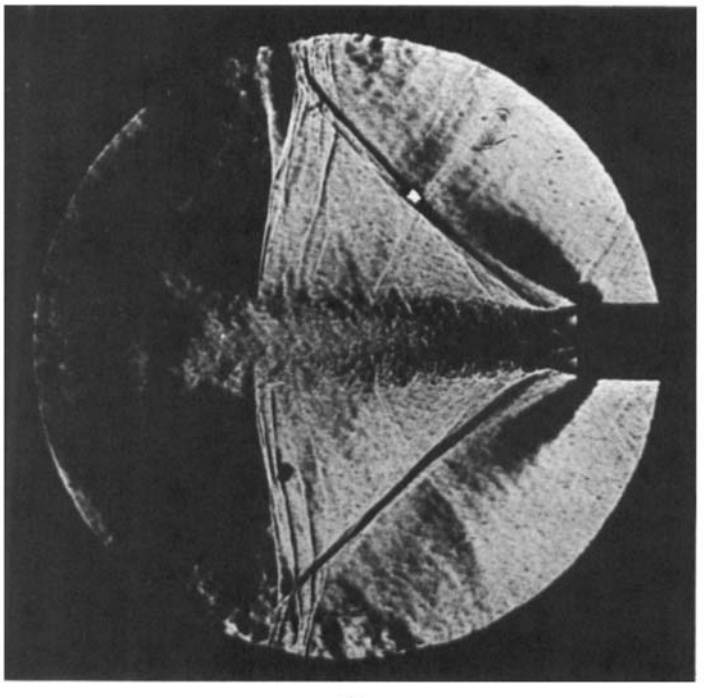

(*d*)

FIGURE 10(*c*, *d*). For legend see p. 283.

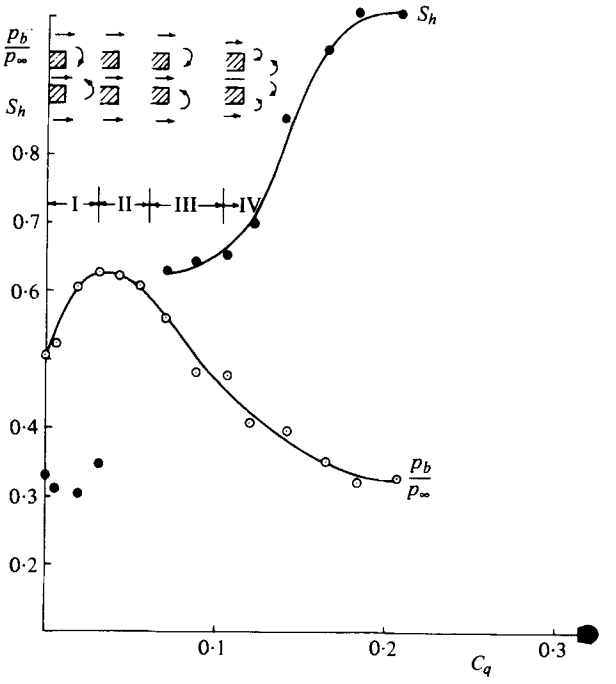

FIGURE 11. Variation of base pressure and Strouhal number with bleed air mass flow for $M_\infty = 1{\cdot}30$.

now two vortex streets symmetrically disposed about the centre-plane of the wake. The signals from a hot-wire traverse show two separate regions of periodicity separated by a region on the wake centre-line in which the flow is turbulent and irregular but not in any sense periodic. Once this flow regime is established further increase in the flow rate of the bleed air produces rapid increase in the frequency of the vortex streets.

Some spark-schlieren photographs illustrating the principal features of the wake flow are presented in figure 10(*a–d*). These photographs were taken at a mainstream Mach number of 1·06 which is slightly different from the Mach number for the results given in figure 9. However, it is not considered that this disparity is significant.

Figure 10(*a*) shows the wake flow for a value of blowing coefficient, C_q, of 0·0092, sufficient to raise the base pressure ratio to just below 0·6. The flow pattern should be compared with that shown in figure 8(*b*) for the case of zero bleed. It is evident that this comparatively small amount of bleed air has effected a major change in the flow pattern in the immediate vicinity of the trailing edge. The region of intersection of the trailing-edge shear layers and the trailing oblique shock waves has been moved substantially rearwards and there is no evidence of vortex motions upstream of this region. It also appears that in the vicinity of the shear layers the shock waves have become diffused into a more continuous compression process.

A schlieren photograph illustrating the vortex-free regime is presented in figure 10(*b*). It shows the relatively weak expansion (and correspondingly reduced deflection of the shear layers) associated with the relatively high base pressure occurring in this regime.

Figure 10(*c*) shows the flow pattern for a value of C_q of 0·13 giving the regime in which a single vortex train appears at higher frequency. This figure exhibits a further

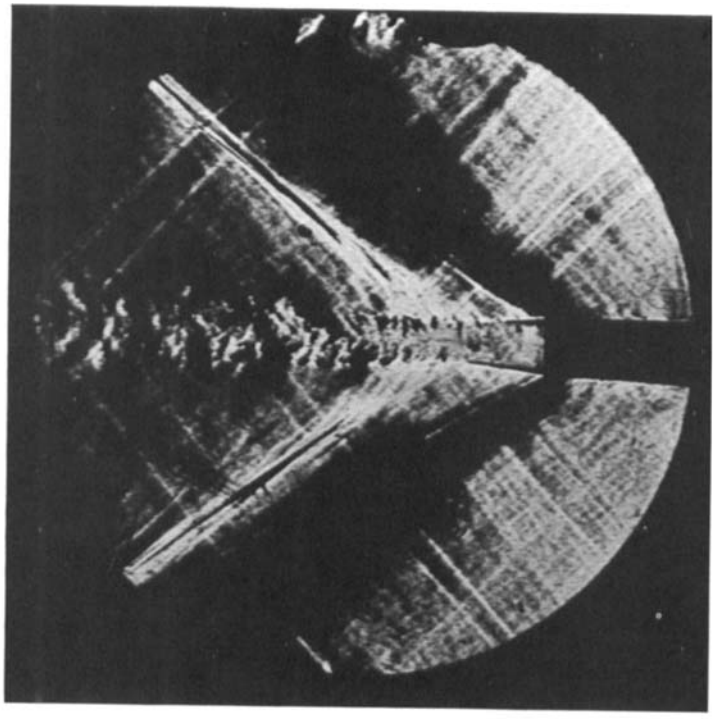

(*a*)

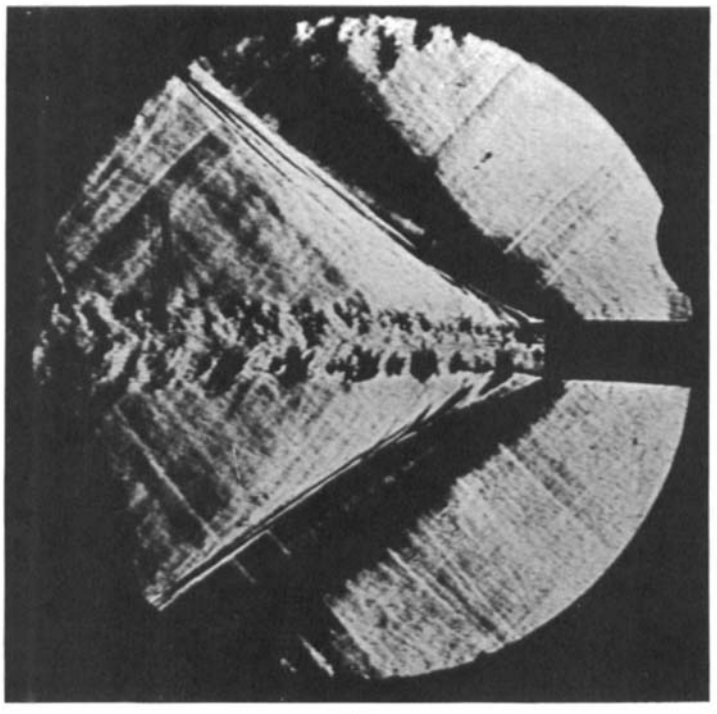

(*b*)

FIGURE 12. Spark-schlieren photographs, $M_\infty = 1{\cdot}30$; (*a*) $C_q = 0{\cdot}019$; (*b*) $C_q = 0{\cdot}089$; (*c*) $C_q = 0{\cdot}21$.

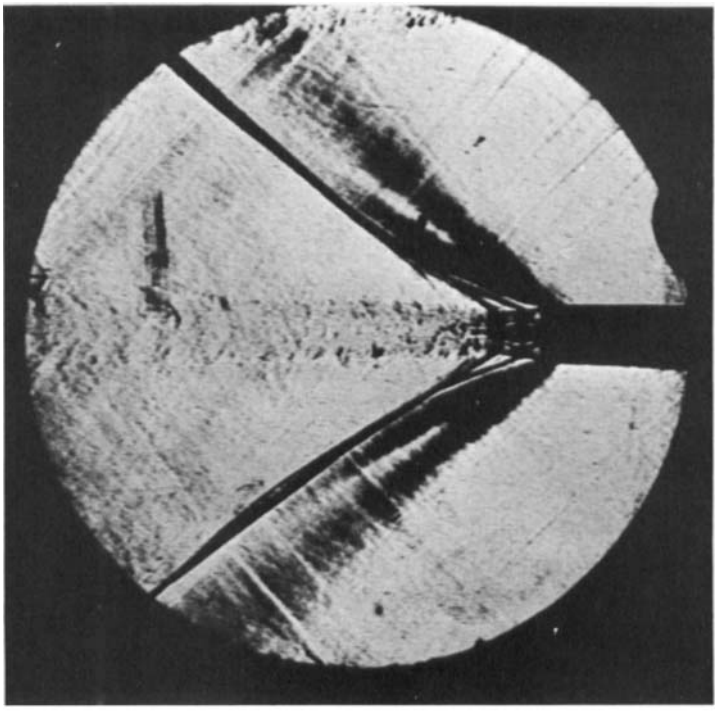

(*c*)

FIGURE 12(*c*). For legend see opposite page.

major change in the nature of the flow in the immediate vicinity of the trailing edge as the two trailing oblique shock waves now spring from points very near to the trailing edge. There is also some evidence in the photograph that the vortices are being shed in symmetrical pairs rather than alternately as in the orthodox vortex street. This has been confirmed by measurements obtained using two photo-multipliers to obtain simultaneous signals from the upper and lower lines of vortices. It appears that the vortices originate immediately behind the solid outer lips of the trailing edge. Vorticity is drawn alternately from the outer shear layer and from the bleed air, which reaches sonic speed in this range of values of C_q.

The regime of the double vortex street is shown in figure 10(*d*) for a value of C_q of 0·2. The stream of bleed air expands to supersonic speed from the face of the slot so that behind the trailing edge on each side of the slot there is a region in which two supersonic shear layers are converging. The trailing oblique shocks spring from points near to the convergence of the shear layers. The figure shows evidence of the two distinct vortex streets separated by the central region of the wake, in which the flow is turbulent but not periodic.

3.3. *Effect of bleed air*, $M_\infty = 1{\cdot}3$

The effect of the rate of mass flow of the bleed air on base pressure and on vortex-shedding frequency is shown in figure 11 for a mainstream Mach number of 1·30. The general features are similar to those shown in figure 9 for transonic flow. However, the maximum value of base pressure is not so high above the zero bleed flow value and the base pressure drops off more rapidly at higher rates of bleed flow. For low rates of bleed the values of Strouhal number are similar to those in the transonic case but at

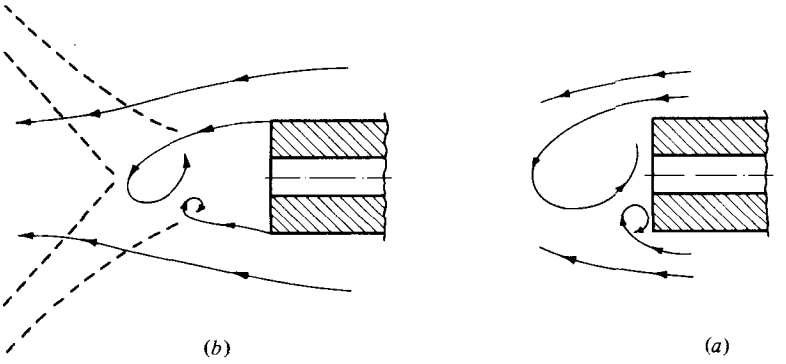

FIGURE 13. Diagrammatic representation of vortex formation. - - -, oblique shock waves.

the point where the vortex motion is reinstated after the base pressure peak the value is significantly higher and the frequencies increase more rapidly with the blowing rate.

Spark-schlieren photographs of the wake flow are given in figures 12(*a–c*). The principal features are similar to those shown in figures 10(*a–d*) for transonic flow though there is less clarity. However, if figure 12(*a*), for $C_q = 0{\cdot}019$, is compared with the result for zero bleed shown in figure 8(*c*) it is observed that the differences are smaller than in the case of transonic flow. This is because, even for the zero blowing case, the region of convergence of the shear layers occurs some distance behind the trailing edge so that the emission of a small amount of bleed air has less effect on the flow in the immediate neighbourhood of the trailing edge. Correspondingly the rise of base pressure which results is small compared with that occurring in the transonic case.

4. Discussion

4.1. *Zero bleed flow*

We consider first the fluid mechanics of the base flow and wake in the absence of bleed flow. The schlieren pictures of figures 8(*a*, *b*) show vortices formed in the immediate vicinity of the face of the trailing edge, the size of the vortices being comparable to the trailing edge thickness. This pattern occurs for mainstream Mach numbers up to about 1·18, corresponding to the minimum value of the curve of base pressure (figure 7). Fluid is not entrained symmetrically into the base region and the train of vortices results from the dominance successively of the upper and lower trailing-edge shear layers. When the dominant vortex behind the trailing edge is being energized by the upper shear layer (figure 13*a*) a smaller vortex of opposite sign will tend to grow near the separation point of the lower shear layer.

For the situation sketched in figure 13(*a*) the effect of the trailing-edge vortex would be to increase the rate of shear in the lower shear layer with, presumably, the resultant effect of increasing the pressure rise from the base region to the downstream wake region and thus of reducing the base pressure. It is relevant that Brogna & Hawks (1978) showed that suction of shear-layer fluid into the base produced a reduction in base pressure.

At higher mainstream speeds the flow immediately behind the trailing edge is different in character as figure 8(*c*) shows for $M_\infty = 1{\cdot}3$. In this case the hot-wire

signals showed periodicity of low amplitude in the base region. The amplitude of the periodic signals increased greatly in the region in which the two trailing oblique shocks converge on the trailing-edge shear layers. It is from this region that air must be returned towards the trailing edge to replace the air entrained by the shear layers. The schlieren picture shows insufficient detail to enable the flow to be accurately visualized. However it may be surmised that the flow is somewhat as shown in figure 13(*b*), in which it is suggested that the change in flow direction does not occur symmetrically but is associated with vortex formation in the region of pressure rise, which would tend to increase the velocity gradients in the shear layers. As a vortex grows in the upper shear layer (as in figure 13*b*) its interaction with the lower shear layer would tend to originate a succeeding vortex of opposite sign.

The interaction with the shear layers in the immediate vicinity of the base (say within one base height) appears to be minimal. It may be noted that the value of p_b/p_∞ for this supersonic case is significantly higher than for the transonic case, at 0·5 against 0·43. The relative frequency of the vortex street is only slightly higher and it therefore appears that the essential difference between the two cases results from the difference in the mechanics of the vortex formation and the distance of the region of vortex formation from the trailing edge. This is the probable explanation for the general rise in the value of p_b/p_∞ shown in figure 7, for $M_\infty > 1{\cdot}18$, and in figure 6 for $M_\infty > 1{\cdot}16$.

The conditions that govern the downstream shift of the zone of vortex formation are not clear. However, for the four experimental points in the range $M_\infty > 1{\cdot}2$ (figure 7) the measured values of frequency lie in the narrow band between 16·8 and 17·2 kHz. At lower Mach numbers the measured frequencies increase from 6·0 kHz at $M_\infty = 0{\cdot}6$ to 16·2 kHz at $M_\infty = 1{\cdot}18$.

The time required for a pressure pulse to travel transversely between the two shear layers at the trailing edge depends on what fraction of the shear layer is traversed. Estimates of the corresponding frequency range between about 23 kHz (for the trailing edge alone) to about 16 kHz if half of each shear layer is included. This evidence suggests that in the lower range of Mach number the frequency is controlled by a mechanism related to the rate of growth of the vortex. It appears that the zone of vortex formation shifts away from the trailing edge at speeds at which the frequency approaches that corresponding to the transverse travel of sound waves.

It is in this region that the most important differences begin to appear between the results for the solid base (figure 6) and the slotted base (figure 7). It may be that these differences arise from the effect of the trailing-edge geometry on the mechanism of vortex formation but there is insufficient evidence to enable a more specific conclusion to be drawn.

4.2. *Effect of bleed air*, $M_\infty = 1{\cdot}03$

It is clear that for mainstream Mach numbers just greater than unity a small amount of bleed air produces a substantial increase in base pressure (regime I in figure 9). The photograph of figure 10(*a*) shows that this is associated with a major change in the character of the flow in the base region, the point of initiation of the vortex train being moved rearwards. A reasonable hypothesis is that, with reference to figure 13(*a*), a small flow of air from the central slot would oppose the motion of the newly forming vortex and prevent its growth. Therefore the vortices do not form in the base region but in the region of pressure rise at the confluence of the trailing oblique shock waves

(figure 10*a*). The mechanism could be similar to that illustrated in figure 13(*b*) and some confirmation is afforded by a comparison of figures 10(*a*) and 8(*c*).

In fact as the blowing rate is increased the point at which periodic signals are first detected has been found to vary more or less linearly with C_q for values of C_q up to 0·04, the distance behind the trailing edge being given (for $M_\infty = 1{\cdot}03$) by

$$\frac{x}{2h} = 250C_q.$$

Thus for $C_q = 0{\cdot}03$ the vortices form at 7·5 times the base height downstream, which is the limit of the field for schlieren photographs. The rise in base pressure is also virtually complete at this point (figure 9) and it seems likely that there is some lower value of C_q at which the influence of the vortex motion becomes small, the base pressure being controlled by the extent to which the entrainment required by the shear layers is supplied by the bleed air so that recirculation in the base region is reduced.

In fact for $0{\cdot}05 < C_q < 0{\cdot}09$ there is no vortex motion. In this regime (II on figure 9) the jet of bleed air penetrates along the centre-line of the wake, separating the two outer shear layers so that they do not interact.

However, vortices are again observed for $C_q > 0{\cdot}09$. It is in this regime (III on figure 9) that the vortices are shed in symmetrical pairs, vorticity being drawn alternately from the outer shear layer and the bleed air. The flow pattern would be similar to that of figure 13(*a*) but with the full trailing edge replaced by the outer lip. This would be consistent with the higher frequencies observed in this regime.

For $C_q = 0{\cdot}14$ the bleed air expands from an approximately sonic value at the slot face to an appreciably supersonic value in the base region and at this and higher values of C_q two vortex streets occur (regime IV of figure 9), separated by a turbulent region along the wake centre-line (figure 10*d*). There is on either side of the central jet a region in which supersonic shear layers are converging and it seems likely that in each of these regions the mechanism of vortex generation is similar to that illustrated in figure 13(*b*). As C_q increases the shear layers from the central jet play an increasingly important role in the vortex formation. For this reason, presumably, there is a rapid increase of Strouhal number with C_q – almost a linear relationship.

Since the experiment has been carried out with a fixed ratio of slot height to base height the effects of momentum flux in the bleed flow could not be separated from the effects of mass flux as represented by the variation of C_q. It seems possible that different slot/base ratios would give similar flow regimes to those observed but with the boundaries between regimes occurring at different values of C_q. For example, regime II occurs when the jet of bleed air penetrates the wake to separate the outer shear layers. It is probable that this effect would be dependent on the jet momentum and it might be expected that a smaller slot, giving higher momentum flux for a given mass flux, would cause regime II to occur at a lower value of C_q. However the full investigation of such effects requires a further series of experiments.

4.3. *Effect of bleed air*, $M_\infty = 1{\cdot}3$

For the case of supersonic mainstream flow ($M_\infty = 1{\cdot}3$) the results shown in figure 11 exhibit the same general features as those of figure 9 for transonic flow. However, at low values of bleed mass flow the two cases are different. For $M_\infty = 1{\cdot}3$ small quan-

tities of bleed air do not radically change the flow in the base region. Figures 8(*c*) and 12(*a*) are rather similar though the region of vortex formation is moved slightly rearwards by the effect of the bleed air. In fact in this regime the effect of the bleed air on the entrainment ratio of the shear layers is probably as important as its effect on the vortex formation.

For $C_q > 0{\cdot}07$ values of Strouhal number are higher than in the transonic case and increase more rapidly with C_q, corresponding to a steeper reduction in base pressure. However the two different vortex regimes already described for the transonic case (and indicated by III and IV on figure 11) may still be identified.

5. Conclusions

Experimental observations have been made of vortices shed from the blunt trailing edge of an aerodynamic body over a range of mainstream Mach numbers from 0·68 to 1·3. The effect of bleed air discharged from a slot in the trailing edge has been examined.

With zero bleed from the slot the increase of mainstream Mach number caused a reduction of non-dimensionalized base pressure (p_b/p_∞) to a minimum value at $M_\infty = 1{\cdot}18$ with a subsequent rise at higher Mach numbers. This rise resulted from a rearward shift of the point of origin of the vortex motion from the immediate vicinity of the trailing edge to the region of confluence of the trailing-edge shear layers. An experiment on a solid (non-slotted) base gave similar results with some differences in detail. In both cases the Strouhal number rose to a maximum value coinciding with the minimum value of base pressure.

At transonic mainstream Mach numbers the effect of a small amount of base bleed was to shift the point of origin of the vortex motion downstream, resulting in a substantial increase in base pressure. The vortex motions disappeared over a range of bleed air mass flows near to the value producing a maximum value of base pressure. At higher bleed rates two different regimes of vortex motion were observed, and the base pressure was reduced again.

For a supersonic mainstream Mach number (1·3) similar phenomena were observed. However, small amounts of bleed air produced a smaller rise in base pressure and higher rates of bleed air mass flow produced a more rapid reduction in base pressure.

The work represents part of a research programme being carried out with support by a Research Grant from the Science Research Council of Great Britain (GR/A51174). This support is gratefully acknowledged.

The authors have benefited greatly from discussions with Dr J. C. Gibbings and Dr J. W. Cleaver whose suggestions have been most helpful. Mr Saad Al-Shukri, a postgraduate student, and Mr Derek Smith, provided valuable help in the development of the hot-wire system.

Mr John Paterson gave invaluable technical assistance, especially in the demanding task of running the transonic tunnel, and Mrs McKinley's help with the photography was also much appreciated.

REFERENCES

ABDUL-KADIR, F. F. 1976 Base pressure effects on aerofoils in transonic flow. Ph.D. thesis, University of Liverpool.

BEARMAN, P. W. 1967 The effect of base bleed on the flow behind a two-dimensional model with a blunt trailing edge. *Aero. Quart.* **18**, 207–224.

BROGNA, S. J. & HAWKS, R. J. 1978 Effect of base suction on subsonic drag of bluff bodies. *J. Aircraft* **15**, no. 7.

EDWARDS, S. J. 1980 The effects of trailing edge coolant on trailing edge losses. M.Eng. thesis, University of Liverpool.

HEINEMANN, H. J. & BÜTEFISCH, K. A. 1978 Determination of the vortex shedding frequency of cascades with different trailing edge thickness. *AGARD Conf. Proc.* no. 227, paper 35.

HEINEMANN, H. J., LAWACZECK, O. & BÜTEFISCH, K. A. 1975 Von Kármán vortices and their frequency determination in the wakes of profiles in the sub- and transonic regimes. *IUTAM Symposium Transonicum II, Göttingen.*

LAWACZECK, O. & HEINEMANN, H. J. 1975 Von Kármán vortex streets in the wakes of subsonic and transonic cascades. *AGARD-PEP-meeting on Unsteady Phenomena in Turbomachinery, Monterey, California, U.S.A.*

MALHOTRA, J. P. 1974 Transonic base flow past blunt trailing edge. M.Eng. thesis, University of Liverpool.

MIKULLA, V. 1969 Hot-wire and film measuring techniques in compressible jet flow. M.Eng. thesis, University of Liverpool.

WOOD, C. J. 1964 The effect of base bleed on a periodic wake. *J. Roy. Aero. Soc.* **68**, 477–482.